

Cite this: *Chem. Commun.*, 2011, **47**, 8730–8739

www.rsc.org/chemcomm

HIGHLIGHT

Smart nanocontainers as depot media for feedback active coatings

Dmitry G. Shchukin* and Helmuth Möhwald

DOI: 10.1039/c1cc13142g

Among the grand challenges at present are ways to develop systems with low consumption of raw materials and with little load on the environment. In view of this it is of utmost importance to avoid or to delay processes causing material destruction. This is especially urgent, since many protective substances have associated health hazards, and new routes to improve the situation are a main concern of this contribution. Nanocapsules (nanocontainers) with controlled release properties of the shell can be used to fabricate a new family of active coatings, with quick response to changes of the coating environment or coating integrity. The release of active materials encapsulated into nanocapsules is triggered by various external and internal factors, thus preventing spontaneous leakage of the active component. The coating can have several active functionalities when several types of nanocapsules loaded with corresponding active agent are incorporated simultaneously into a coating matrix. We highlight recent achievements in development and application of filled responsive containers in biomedical and self-healing protective coatings.

Department of Interfaces,
Max-Planck Institute of Colloids and
Interfaces, D14424 Potsdam, Germany.
E-mail: dmitry.shchukin@mpikg.mpg.de;
Fax: +49-331-567-9202;
Tel: +49-331-567-9781

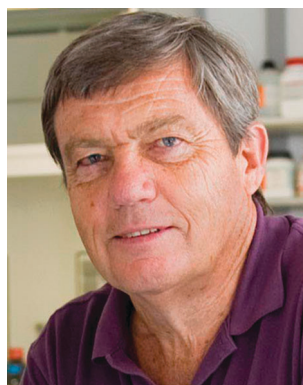
Development of a new generation of
multifunctional coatings and films, which
possess not only passive functionality but
also active and rapid feedback activity in
response to changes in local environment, is

a key technology for fabrication of future
high-tech products with multifunctional
surfaces. These coatings should have
not only passive properties inherited
from “classical” approaches (e.g., barrier,

**Dmitry G. Shchukin**

Dmitry Shchukin is currently a group leader at the Department of Interfaces, Max Planck Institute of Colloids and Interfaces, Potsdam, Germany. He obtained his PhD in physical chemistry (2002). He has received a DAAD fellowship (2001), Alexander von Humboldt fellowship (2004), and Incoming Marie-Curie fellowship (2005) at the Max Planck Institute of Colloids and Interfaces. He was awarded the NanoFutur Price (2006) and ForMaT Price (2010) of the

German Ministry of Education and Research. His main scientific interests concern the fabrication of hollow nanocontainers and development of feedback active coatings, study of chemical and physico-chemical processes in confined nanoenvironment, and interfacial sonochemistry.

**Helmuth Möhwald**

Helmuth Möhwald received his diploma in physics (1971) and PhD (1974) from Univ. Göttingen (Germany) for research in organic solids. After a postdoc at IBM San Jose, as assistant Professor at Univ. Ulm, and as a research scientist at Dornier Systems, he became associate professor in biophysics at TU Munich (1981). From a chair in physical chemistry at Univ. Mainz (1987) he became founding director of the Max Planck Institute of Colloids and Inter-

faces in Potsdam (1993). His recent honours have been the Overbeek medal, the Gay-Lussac–Humboldt award (2007), an honorary doctorate of Univ. Montpellier (2008) and the Wolfgang-Ostwald award (2009).

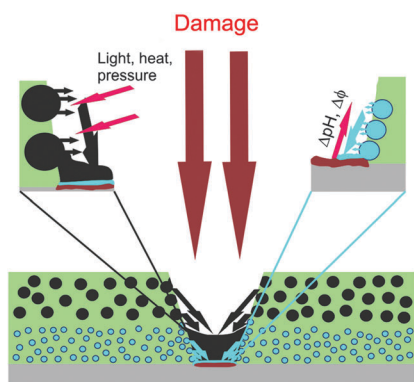


Fig. 1 Schematic representation of nano-capsule-based self-healing coatings.³

color, adhesion) but also active functionality, which provides fast and, if necessary, reversible response of the coating performance to instant or gradual impacts occurring either in the coating body (e.g., cracks, local pH change, bacterial activity) or in the environment surrounding the coating (e.g., changes of the temperature, illumination, humidity). Ideally the coatings should also have several passive and active functionalities (e.g., antireflection, antifungal and anticorrosion) exhibiting synergistic effects, rendering the surface of any coated substrate functional and responsive.

To provide sustained or immediate release of the functional material on demand, the active part of the coating has to be incorporated into a passive matrix or form a layered structure together with the passive matrix. Recent developments in surface science and technology provide new opportunities of modern engineering concepts for fabrication of active feedback coatings, through the integration of nanoscale layers (carriers) loaded with active compounds (e.g., inhibitor, lubricant, drug, vitamin) into existing “classical” films, thus designing completely new coating systems of the “passive” host–“active” guest structure.

The most important factor in the design of new active films is to develop depot systems incorporated into the coating matrix. There are several approaches demonstrated so far for the design of such depot systems: (i) polymer containers,¹ (ii) polymer or glass fibres,² (iii) nanocontainers with polyelectrolyte shell,³ layered double hydroxides, and mesoporous inorganic materials,⁴ and, finally, design of the coatings employing polyelectrolyte

multilayers by layer-by-layer assembly (LbL).⁵ All of the mentioned methods have specific advantages and drawbacks concerning the upscaling possibility, performance, feasibility to employ different active materials, *etc.*, whose detailed description lies out of the scope of the present paper. This Highlight mainly focuses on the coatings with active material entrapped in nanocapsule depots, thus providing in our opinion, the highest versatility of the coating functionality in the terms of encapsulated active agent, combined with very good upscaling possibility.

The key idea behind this approach is to create nanocontainers for loading of active agents with shells possessing controlled permeability specific to several triggers, and then to introduce them into the coating matrix (Fig. 1). Being uniformly distributed in the passive matrix, these nanocontainers will keep the active material in a “trapped” state avoiding undesirable interaction between the active component and the matrix, as well as preventing spontaneous leakage. If the local environment undergoes changes or if the active surface is affected by outer impact, the nanocontainers respond to this stimulus and release encapsulated active material.

The use of different types of micro- and nanocapsules for encapsulation, controlled delivery and release of active materials has become increasingly popular. For example, micron sized capsules with layer-by-layer assembled polyelectrolyte shells are used for encapsulation and release of drugs, DNA, dendrimers and enzymes;^{6–8} inorganic halloysite nanotubes were demonstrated to be suitable for loading of ferments and inorganic nanoparticles.^{9,10} Hydrogels were used for encapsulation of phospholipids, drugs, as liposome reactors and plant growth media.^{11,12} There are numerous publications on the application of micelles and microemulsions in delivery systems and we will address several recent reviews to provide better understanding of the current achievements in the use of micelles and microemulsions for encapsulation.^{13,14}

An important step in fabrication of nanocapsules for feedback active coatings is to make the capsule shell sensitive to impacts from the environment or to distortion of the coating integrity.

This task can be achieved by employing the weak forces between the shell components during shell formation: electrostatic, pH-bonding, supramolecular or hydrophobic forces in a layer-by-layer deposition.¹⁵ The procedure consists in construction of the nanocontainer shell by layer-by-layer deposition of oppositely interacting species (e.g., polyelectrolytes, nanoparticles, biomaterials) on the surface of capsule scaffold (mesoporous oxide nanoparticle, polymer shell, *etc.*).¹⁶

The controlled release/upload of the capsules is, in general, dependent on the interaction between the material of the shell and the environment surrounding the container. The shell of the containers should selectively react only to one or two triggers, changing its permeability, while the others should keep the shell intact. The following triggers could be utilized for opening/closing of the container shell: local pH changes, temperature changes, electromagnetic irradiation, mechanical pressure (also ultrasonic treatment), humidity, electric (electrochemical) potential, ionic strength and dielectric permeability of the solvent. The simplest trigger for opening/closing of the capsule shell is pH shift in the local environment. Polyelectrolyte capsules, hydrogels and emulsions with weak acidic or basic functional groups in the shell are sensitive to pH, demonstrating reversible and (or) irreversible changes of the shell permeability in a wide pH range (e.g., at low pH < 4 or high pH > 9).^{17,18} For response to electromagnetic irradiation, the capsule shell should have sensitive components, for example, metal (silver) nanoparticles, for IR light,¹⁹ dyes for visible light,²⁰ and semiconductors for UV light absorption.²¹ Mechanical impact activation requires a certain level of rigidity or brittleness of the shell because the elastic shell should undergo deformation under pressure but not rupture;²² containers with diameter < 100 nm are rarely destroyed with reasonable mechanical force because they tend to escape from the force direction.

Polyelectrolyte capsules composed of poly(allylamine)/poly(styrene sulfonate) multilayers preserve their integrity after heating at 120 °C for 20 min in aqueous solution but show a considerable decrease in size (50–70% depending on the diameter of the initial capsules).²³

The diameter decrease is accompanied by a strong increase of layer thickness and decrease of permeability, which lead to enhanced entrapment capabilities and the capsules become impermeable even for small molecular weight compounds. The driving force for this polyelectrolyte rearrangement process is the entropy gain of the more coiled state of the polyions and the decreased interface between polyelectrolytes and water. Probably some water, which fills the pores of the multilayers, is expelled during temperature treatment. Other triggers for capsule opening, such as high ionic strength of the solvent²⁴ or changes of the electrochemical potential of the coating²⁵ are usually involved in feedback active systems of specific functionality, and so far have yet to find broad potential applications.

Summarizing the state-of-the-art of nanocapsule-based active coatings, two main application areas can be emphasized: (i) various self-healing protective coatings (primarily anticorrosion coatings) and (ii) bioactive coatings, and most publications up to date are devoted to them.

Self-healing protective coatings

Microencapsulated (dicyclopentadiene) healing agent and highly-porous Ru catalyst were incorporated into an epoxy matrix to produce a polymer composite capable of self-healing (Fig. 2).²⁶ Both the pristine and healed fracture toughness depend strongly on the size and concentration of microcapsules added to the epoxy resin.

Addition of dicyclopentadiene-filled urea-formaldehyde microcapsules into

epoxy samples yields up to 127% increase in coating toughness. The increased toughening associated with fluid-filled microcapsules is attributed to the healing of subsurface microcracking. Overall the embedded microcapsules provide two independent effects: the increase in pristine fracture toughness from general toughening and the ability to self-heal the pristine fracture event. Healed fracture toughness increases steadily with microcapsule concentration until reaching a plateau at about 20 vol%. The maximum healing efficiency for 180 μm diameter microcapsules occurs at low concentrations (5 vol%). For 50 μm microcapsules, high healing efficiency only occurs at higher microcapsule concentrations (20 vol%) since more capsules are required to deliver the same volume of healing agent to the fracture plane. Diene monomers (dicyclopentadiene and 5-ethylidene-2-norbornene, *etc.*) and their blends were investigated as candidate self-healing agents with Grubbs catalyst.²⁷ It was found that the reaction becomes faster with increase of 5-ethylidene-2-norbornene content at lower catalyst loading. Rigidity after 120 min cure was the highest in a dicyclopentadiene : 5-ethylidene-2-norbornene blend when it was cured on the epoxy resin coating. Considering requirements for effective self-healing (*i.e.*, fast reaction during cure, high rigidity after cure, reduction of catalyst amount, and lower temperature capabilities), dicyclopentadiene and 5-ethylidene-2-norbornene blends are good potential candidates for self-healing agents. The proposed self-repairing approach had, however, some essential drawbacks for application in protective self-healing coatings: (i) the concentration of Grubbs' catalyst has

to be quite high, increasing the price of the coating, especially in the case of large surfaces to be protected; (ii) inherent shortcomings of the method based on diene monomers are potential side reactions with the polymer matrix and air; (iii) the relatively large size of capsules (50–200 μm) inhibits their application to coatings with thickness less than 0.5 mm because of integrity failure. On the other hand, lowering the microcapsule size without reduction of self-healing efficiency requires much higher concentration in the coating matrix. Samples with smaller microcapsules must have very good adhesion to the epoxy matrix to ensure capsule rupture under stress.

Urea-formaldehyde microcapsules filled with drying linseed oil were used for the healing of cracks in an epoxy coating.²⁸ Microcapsules were synthesized by *in situ* polymerization in an o/w-emulsion. Initially fully water-compatible urea and formaldehyde react in continuous aqueous medium to form poly(urea-formaldehyde). As the molecular weight of this polymer increases, the fraction of polar groups gradually decreases till the polymer molecules become hydrophobic and get deposited on the surface of o/w-emulsion droplets. The obtained microcapsules were then incorporated in an epoxy resin coating. Since the outer shell surface of the microcapsules was very rough, strong binding to the coating matrix was provided.

The encapsulated linseed oil is released by coating cracks and fills the cracks in a coating matrix (Fig. 3). Finally, oxidation of linseed oil by atmospheric oxygen leads to the formation of a continuous film inside the crack. Superior corrosion resistance of such a self-healing coating was demonstrated by comparative exposure of two specimens in a salt spray cabinet. The sample coated by a film containing capsules remained free from corrosion at an artificial scratch up to 72 h of exposure. In contrast, the control specimen suffered from corrosion already after 48 h.

A composite metal coating with organic liquid-containing microcapsules obtained by electroplating of a metal substrate was chosen in order to achieve the sustained release of a liquid lubricant, lowering the friction between repeatedly contacting surfaces (self-lubricating coating).²⁹

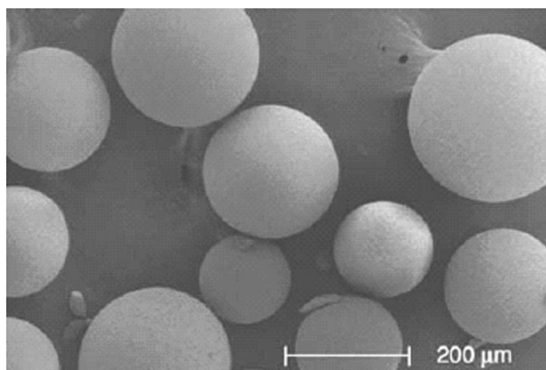


Fig. 2 Urea-formaldehyde microcapsules containing dicyclopentadiene.²⁶



Fig. 3 Microscope photos of self-healing coating films with urea–formaldehyde microcapsules immediately after crack formation (left) and after 90 s (right).²⁸

Microcapsules with liquid organosilica resin as the core and poly(vinyl alcohol) as the shell material were prepared *via* o/w emulsification using an alkyl polyoxyethylene polyether type surfactant as a stabilizer. Subsequent electroplating from a mixture of electrolyte solution and capsule dispersion achieves the formation of composite capsule-containing metal coating. When the samples were subjected to a scratch or wear test, surface wetting in the immediate vicinity of the damaged site was observed, confirming the release of liquid from the broken microcapsules and the ability of coating to lead to self-lubrication.

Organosiloxanes form covalent bonds with the surface of metal substrates bearing hydroxyl groups and impart coupling (in case of usual siloxanes) or water-repelling (for long-chain terminated siloxanes) functionality to it.³⁰ Moreover, organosiloxanes with multiple SiOR moieties can undergo a lateral polycondensation reaction at the substrate surface, forming a 2D network with excellent protective ability against corrosion. These properties of organosiloxanes were taken into account by Latnikova and co-workers³¹ where the authors proposed to encapsulate a mixture of emulsified organosiloxanes and then incorporate them into the coating matrix. Micro- and nanocontainers with core-shell morphology and polyurethane/polyurea shells were successfully synthesized by emulsion interfacial polyaddition and then embedded in the corrosion protective coating on the epoxy basis. The active part consists of the polyurethane microcontainers loaded with alkoxy silanes with long hydrophobic tails. High efficiency of the coating is achieved by the combination of passivating and water-repelling properties of the loaded material. Moreover, the use of

specially selected alkoxy silanes with functional groups having targeting affinity to the compounds of the coating matrix can provide an excellent adhesion, and therefore coupling functionality between the metal substrate and organic coating matrix.³⁰

When the integrity of the coating is damaged, containers open and their content flows into the crack and spreads on the substrate surface. Exposure to an aggressive ambient medium with high humidity initiates the reaction of the alkoxy silanes with hydroxyl groups on the substrate surface. Finally a highly hydrophobic film is created, resulting in passivation of the substrate surface and water-repelling properties of the damaged area.

The current density maps taken by the local scanning vibrating electrode technique (SVET) immediately, 1 and 12 h after immersion in 0.1 M NaCl are presented for a control sample (Fig. 4c–e) and sample covered with epoxy film containing 6 wt% microcontainers (Fig. 4f–h). A rapid increase of current density with time for the control sample can be observed. At the same time significant suppression of the corrosion process for samples with embedded microcontainers is encountered. The visual corrosion test also clearly confirms the effectiveness of the proposed self-healing system. All control samples showed onset of corrosion already 6 h after immersion in 0.1 M NaCl solution (the process starts with the blackening of the defect surface followed by the appearance of a white fluffy precipitate within the groove of the scratched regions). In contrast, the self-healing samples show no visual evidence of corrosion even 3 days after exposure (the surface of the scratch remains shiny) (Fig. 4a and b).

Deposition of a multilayer poly-electrolyte shell by the LbL approach

directly on the liquid oil core was performed.³² Experimental data obtained for the model oil-in-water emulsion confirm unambiguously the alternating polyelectrolyte assembly in the capsule shell as well as the maintenance of the liquid colloidal core. The obtained microcontainers were stable in the aqueous dispersion for long time, however they reveal quick rupture at the interface due to action of capillary forces. Two different mechanisms of capsule destruction were observed: (1)—the capsule is suddenly burst and the capsule load forms an oily spot around the place where the capsule was situated before. The fast mechanism of capsule destruction is, in our opinion, only possible when the formed polyelectrolyte shell is not homogeneous and has some significant defects. (2)—slow mechanism of capsule destruction due to interaction with the oppositely charged substrate. In this case, the capsule shrinks gradually showing with time more and more concave sites, but remains intact before complete destruction of the shell. The observed fragility of these containers restricts their application especially for their embedment into hard and tough polymeric coatings. On the other hand, slow curing of organic coating formulations containing solvents with similar values of surface (interface tension) can lead to the container's survival and make them potential carriers for loading.

Most of the presented self-healing coatings based on encapsulated oil core–organic shell containers release the active material upon mechanical damage of the shell. So, the next promising step is to proceed towards another trigger of a chemical nature, which affects the permeability of the nanocapsule. The stimuli are, predominantly, concentration of the corrosive species, pH and electrochemical potential. To improve the corrosion protection properties of sol-gel derived hybrid coatings on an aluminum alloy, two organic corrosion inhibitors (mercaptobenzothiazole and mercaptobenzimidazole) have been encapsulated within the coating matrix, in either the presence or absence of cyclodextrin.³³ Superior corrosion protection properties have been found for formulations that contain β -cyclodextrin and can be explained by the slow release of the inhibitor from the cyclodextrin/inhibitor

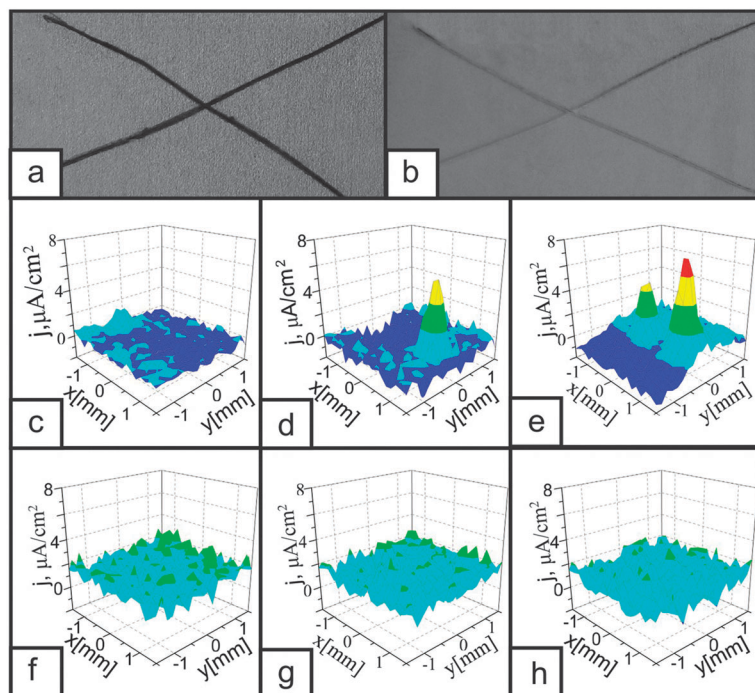


Fig. 4 (a, b) Optical images after 12 h of immersion in 0.1 M NaCl of (a) Al alloy covered with epoxy coating, (b) self-healing of epoxy coating and 6 wt% microcapsules loaded with alkoxy silanes. (c–h) Current density maps after 0 (c, f), 1 (d, g) and 12 (e, h) h of immersion in 0.1 M NaCl for control sample (above) and self-healing system (below).³¹

inclusion complexes and by the self-healing of corrosion defects. The inclusion complexes are more easily trapped within the cross-linked coating material so reducing leaching of the inhibitor.

Deposition of polyelectrolyte multilayers *via* layer-by-layer assembly onto emulsion droplets can be also achieved for droplets of Pickering emulsions as initial templates, yielding finally

microcontainers with significantly improved stability.³⁴ Similar containers were used by Haase *et al.* for loading of the corrosion inhibitor 8-hydroxyquinoline (8-HQ) in their interior.^{35,36} In this case the active agent 8-HQ played simultaneously the role of the hydrophobizing agent for silica nanoparticles forming the container shells. Droplets of diethyl phthalate (oil phase) act as reservoirs for 8-hydroxyquinoline, which is used as (a) the hydrophobizing agent for the silica particles and (b) an encapsulated corrosion inhibitor for application in active feedback coatings. The hydrophobization of silica nanoparticles with 8-HQ is determined by the amount of this agent adsorbed on the nanoparticle surface. The latter is governed by the 8-HQ concentration in the aqueous phase, which, in turn, depends on the degree of protonation and finally on the pH.

The images in Fig. 5a at pH 4.7 clearly show aggregated silica structures on the droplet surface. For pH 4.5 (Fig. 5b), the same effect can be observed but to a slightly lower extent. Droplets at pH 4.2 (Fig. 5c) show incomplete monolayer coverage with some unoccupied regions on the diethylphthalate/water interface. Here, the particle hydrophobicity is already insufficient due to the formation of an 8-HQ bilayer and particles begin to repel each other.

The emulsification is reversible upon changing the pH to a value beyond the stability region. The formed emulsions are stable for at least 6 months (for pH 4.5) of laboratory storage without any observation of coalescence. Another important question is whether the destabilization of a stable emulsion can be triggered by a change in pH. 8HQ is amphoteric and its charge and solubility increase in the ranges of low and high pH values (<4 and >9). This leads to enhanced electrostatic repulsion between molecules on the particles surface and, finally, to distortion of the particulate shells around Pickering emulsion droplets. This process does not occur immediately, but after stirring for 1 h both separated phases are obtained. This, in turn, causes the breakup of containers and release of the encapsulated inhibitor while the Pickering emulsions contain 16 wt% of the encapsulated corrosion inhibitor.

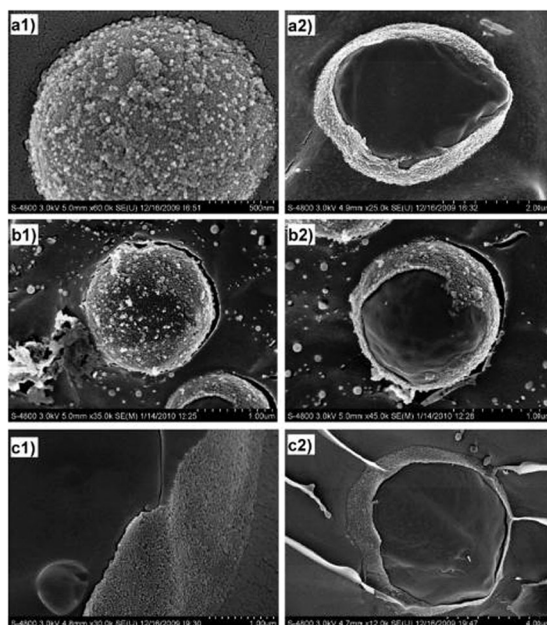


Fig. 5 Cryo SEM images of silica-stabilized emulsion droplets (16.5 wt% 8-HQ) at (a1, a2) pH 4.7, (b1, b2) pH 4.5 and (c1, c2) pH 4.2; cross-section views of droplets are a consequence of the freeze fracture sample preparation.³⁵

Strong self-healing and long-term active corrosion protection of aluminium was shown for benzotriazole-loaded SiO_2 nanocontainers impregnated into a $\text{ZrO}_x/\text{SiO}_x$ hybrid film.^{37,38} To produce SiO_2 nanocontainers for loading into a silica–zirconia hybrid film, the LbL deposition procedure was employed involving both large polyelectrolyte molecules and small benzotriazole ones. The suspension of silica nanoparticles with benzotriazole-loaded polyelectrolyte shell is mixed following the sol–gel protocol and is deposited onto an aluminium alloy by a dip-coating procedure. The uniformly distributed nanoparticles with diameters of about 100 nm are impregnated into the sol–gel film formed on the aluminium substrate with average concentration of the nanocontainers *ca.* $10 \mu\text{m}^{-2}$ of the metal surface. AFM does not show any signs of nanocontainer agglomeration.

Optical photos of the two aluminum samples (Fig. 6) show the drastic difference between the nanocontainer-impregnated and the initial sol–gel film. Many pit-like defects formed on the surface were found after aging even in diluted (0.005 M) NaCl solution for a pure sol–gel film. The film with nanocontainers does not exhibit any visible signs of corrosion attack even after 14 days in 100 times more concentrated (0.5 M) NaCl solution. This pronounced difference shows the advantages of the “nanocontainer” approach over the

direct introduction of inhibitor to the sol–gel coating.

The self-healing efficiency of the $\text{ZrO}_x/\text{SiO}_x$ films impregnated with inhibitor-loaded nanocontainers was also demonstrated by SVET. Artificial defects were formed and well defined cathodic activity appeared at the location of the induced defect on aluminium coated with undoped sol–gel film. Impressively different behavior was revealed after defect formation on the substrate coated with $\text{ZrO}_x/\text{SiO}_x$ film doped by benzotriazole-loaded nanocontainers. No corrosion activity appears in this case after 4 h following the defect formation. Only after about 24 h does a well defined cathodic activity appear in the zone of the induced defect. However, the defect becomes passivated again 2 h later. The most probable mechanism is the following. When the corrosion processes are started, the pH value is changed in the neighboring area, which opens the polyelectrolyte shell of the nanocontainers in a local area, followed by the release of benzotriazole. Then, the released inhibitor suppresses the corrosion activity and the pH value recovers, closing the polyelectrolyte shell of nanocontainers and terminating further release of the inhibitor.

Another possible variant of nanoscale containers demonstrated for feedback active coatings are halloysite nanotubes. Halloysite is an economically viable raw material with kaoline-like composition that can be mined as a raw mineral.³⁹ As for most natural materials, the size of halloysite particle varies within 1–15 μm length and 10–100 nm inner diameter, depending on the deposits. Embedding of the corrosion inhibitor (for example, benzotriazole) inside the inner volume of the halloysite nanotubes was performed according to the adapted procedure described by Price and co-workers.⁴⁰ To attain controlled release properties in the halloysite nanotubes, the surface of the nanotubes could be modified by LbL deposition of polyelectrolyte bilayers.^{41–43} A sol–gel coating impregnated with benzotriazole-loaded halloysites exhibits superior anticorrosion efficiency, which is visible from the practical absence of anodic activity on SVET maps. It is deduced from SVET measurements that during the corrosion process that corrosion centers appear in all samples.

Highest corrosion occurs in the case of bare Al alloy followed by the sol–gel coated sample and the highest protection is provided by the halloysite loaded sol–gel film.

Monodisperse, mesoporous silica nanoparticles were loaded with corrosion inhibitor benzotriazole (BTA) and embedded in a hybrid $\text{SiO}_x/\text{ZrO}_x$ sol–gel coating for corrosion protection of aluminium alloy.⁴⁴ The developed porous system of mechanically stable silica nanoparticles exhibits high surface area ($\sim 1000 \text{ m}^2 \text{ g}^{-1}$), narrow pore size distribution ($d \sim 3 \text{ nm}$) and large pore volume ($\sim 1 \text{ mL g}^{-1}$). As a result, a sufficiently high uptake and storage of the corrosion inhibitor in the mesoporous nanocontainers was achieved. The SEM and TEM images (Fig. 7) reveal a well-developed pore structure with a diameter of 70–90 nm. In all particles, the pores are open, not ordered and oriented from the centre to the outer surface, building a complex worm-like pore system.

A loading capacity of 409 mg (BTA) per 1 g of SiO_2 was found. Assuming that only the pores are filled with the benzotriazole molecules with a molar volume 87.6 mL mol^{-1} , the maximum theoretical loading capacity is $1.53 \text{ g(BTA)/g(SiO}_2\text{)}$. The achieved experimental loading is around one third of the maximum, and is therefore reasonable, but could be further optimized.

The successful embedding and homogeneous distribution of the BTA loaded monodisperse silica nanocontainers in the passive anti-corrosive $\text{SiO}_x/\text{ZrO}_x$ film improve the wet corrosion resistance of the aluminium alloy AA2024 in 0.1 M sodium chloride solution. The anti-corrosive system consisting of a $\text{SiO}_x/\text{ZrO}_x$ film containing BTA loaded SiO_2 -nanocontainers reveals no signs of corrosion even after 10 days of submersion in 0.1 M NaCl. This clear difference from the other samples, alongside the absence of any corrosion induced defects, confirms the high anti-corrosion efficiency of such active, hybrid coatings incorporating inhibitor loaded mesoporous silica nanocontainers. Similar observations were also made by the SVET method.

The next step in the fabrication of ceramic nanocontainers is the formation of a polyelectrolyte shell on their surface after inhibitor loading.⁴⁵ It was shown

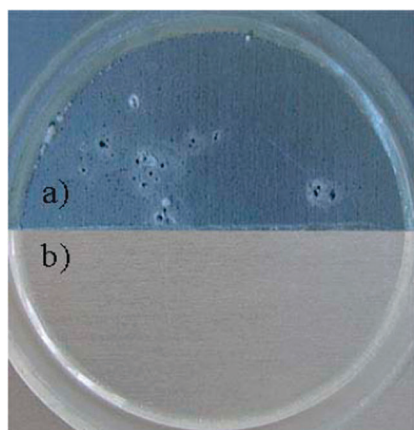


Fig. 6 AA2024 aluminum alloy coated with a sol–gel film directly doped with benzotriazole (a) and with sol–gel film doped with nanocontainers (b) after 14 days of immersion in 0.005 M NaCl (a) and 0.5 M NaCl (b).³⁸

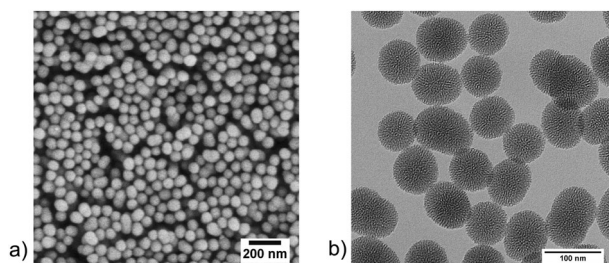


Fig. 7 (a) SEM and (b) TEM micrograph of mesoporous silica nanoparticles.⁴⁴

that a layer-by-layer assembled shell can provide controlled inhibitor release in response to local pH changes and thereby enhanced corrosion protection. The fabrication of a polyelectrolyte shell around the container can be done by layer-by-layer assembly of poly-(allylamine hydrochloride) and poly-(styrene sulfonate), and allows one to prevent the spontaneous release of loaded corrosion inhibitor.⁴⁶ The precision of one adsorbed layer thickness is about 2 nm; further, polyelectrolyte nanocontainers completely repeat the shape of the templating colloids. The opening of the shell can be induced only by changing the surrounding pH value to the alkaline region, while in neutral pH the polyelectrolyte shell remains intact,

preventing undesirable leakage of the entrapped inhibitor.

Tailored mesoporous silica nanoparticles⁴⁷ are quickly becoming the delivery agent of choice for various applications in non-aqueous media.⁴⁸ Therefore, mesoporous silica nanoparticles were synthesized and functionalized with octyl groups on their outer surfaces for better dispersibility into the oil-based coating matrix.⁴⁹ The resultant hybrid coatings were applied to a galvanized steel surface. When intact, they are found to present a layer impregnable to chloride attack for at least a month, and when scratched, strongly impede nascent corrosion processes. The doping of corrosion inhibitor directly into the coating (without nanocapsules) is found

to provide comparatively poor performance even when a tenfold higher concentration of BTA is used. An average intensity-weighted hydrodynamic diameter of ~ 200 nm was obtained for nanocontainers in ethanol, butyl glycol, 1,2-propylene carbonate, with a similar distribution. The addition of a non-polar solvent (xylene) to butyl glycol (intermediate polarity) results in slightly more extensive flocculation, as shown by the shift in average diameter to approximately 350 nm, although the system remains generally stable.

To form the hybrid coatings, a solution of inhibitor-loaded nanocapsules (10 mg BTA per g of nanocontainers) dispersed in butyl glycol was added directly into the oil-based clear coat primer. Due to its high viscosity, this method ensured facile and homogenous dispersion of nanocontainers which were stable for more than 1 month.

Two SVET profiles are shown in Fig. 8a and b for the pure coating and coating with loaded nanocontainers (*i.e.* 2 wt% of nanocontainers in the coating). A clear difference is seen both in these images and in the current density profiles of the control and the sample coated with BTA-loaded nanocontainers, with a much lower measured current above the defect in the latter case. For the control sample, the anodic current rises linearly with time, reaching approximately 0.45 mA after 6 h. In the case of coating with BTA-loaded nanocontainers, a test was carried out for 12 h showing only a gradual increase in anodic current to 0.04 mA. Electrochemical impedance spectroscopy measurements, summarised in Fig. 8c, were carried out alongside short-term corrosion tests (4 days). The doping of BTA directly into the primer adversely affects adhesion due to preferential adsorption of the inhibitor directly to the steel surface during the dip-coating procedure. Such a situation would decrease corrosion protection because of an increased corrosion agent concentration underneath the coating surface. Optical images show the corrosion area for both samples to be enlarged away from the scratch, supporting this argument (Fig. 8d, ii,iii). Optical (Fig. 8d iv,v) images of a coating with BTA-loaded nanocontainers show a very small build up of corrosion products compared to

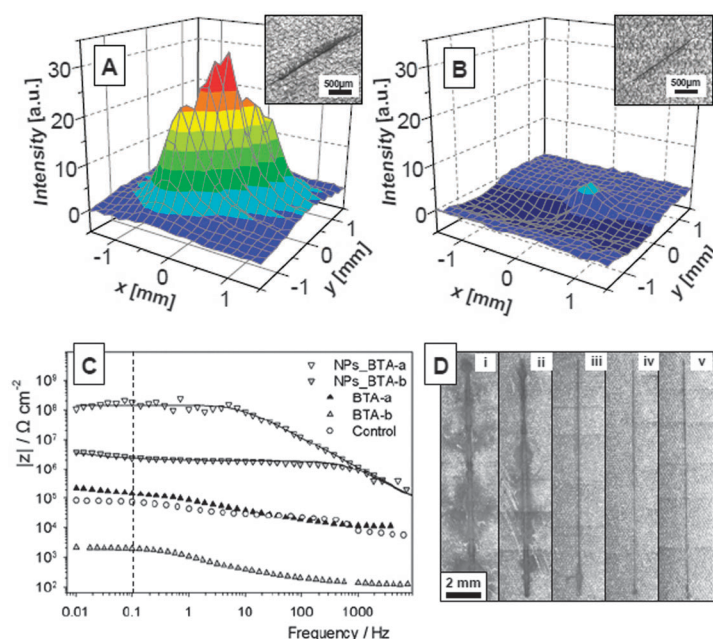


Fig. 8 SVET current density map and (inset) visual appearance of the scratched clear coating (a) and coating with BTA-loaded nanocontainers (b) after 6 h immersion in 0.1 M NaCl. (c): Bode plots of the scratched samples after 4 days immersion in 0.1 M NaCl. (d) Appearance of the samples after 4 days immersion in 0.1 M NaCl. (i) control – clear coating; (ii) BTA-b and (iii) BTA-a coatings with direct doping of BTA with 0.27 and 2.7 mg g⁻¹, respectively; NPs of BTA-b (iv) and BTA-a (v) coatings with BTA loaded nanocontainers with total BTA concentration of 0.2 and 0.1 mg g⁻¹, respectively.⁴⁹

that for the control or directly-doped samples. No problems were noted with the hybrid coating adhesion. The combination of these factors when using 2 wt% content of inhibitor-loaded nanocontainers is sufficient to return the coating performance almost back to that of the intact control sample.

Bioactive coatings

The active coatings based on loaded capsules open a new approach in the development of a new generation of coatings and films in medicine. Because the coatings require direct contact with the tissue to respond to the external trigger and to produce a biomedical effect, their main fields of application are curing of skin and modification of an implant surface. Formation of nanocontainer-loaded bioactive films on the surface of plasters, bandages or implants will result in continuous or dosed release of active substances on the wound. The release can be regulated either by pH, antibodies and ferments inside the wound or by external local heating or microwave irradiation.

Composite nanofilms of stabilized large unilamellar liposomes have multilayer architecture formed by the layer-by-layer assembly from two biocompatible polyelectrolytes, hyaluronic acid and poly-L-lysine (HA and PLL) in NaCl solution, onto which phospholipid liposome "interlayers" were adsorbed and subsequently embedded by further polyelectrolyte adsorption.⁵⁰ Carboxy-fluorescein encapsulated in the vesicles remains inside without sustained release at room temperature indicating that the

liposomes stay intact upon immobilization. The encapsulated dye can be released in a controlled manner by a temperature increase above the main phase transition temperature of the lipid mixture used to prepare the vesicles, found to be 34 °C. However, for the practical application of these specific composite nanofilms in medicine the temperature triggering the release of active compounds has to be increased towards the normal temperature of the human body. This could be achieved *via* suitable lipid mixtures.

DNA-grafted poly(*N*-isopropylacrylamide) (PNIPAM) micelles were assembled into multilayered thin films, and subsequently functionalized by poly(ethylene glycol) (PEG).⁵¹ The presence of PNIPAM within the DNA-polymer hybrid film reduces the permeability of the microcapsules to macromolecules (*e.g.*, dextran) as compared with microcapsules made solely of DNA. A reagentless enzymatic sensor based on the controlled delivery of a reactant was developed by incorporation of luciferin in the structure of acrylic microspheres subsequently confined in a photopolymerized poly(vinyl alcohol) film.⁵² The self-containment working time is estimated to be 2.5 h in the case of the monoenzymatic biosensor for ATP and 3 h for continuous assays for ATP, ADP and AMP, when using the biosensor equipped with the compartmentalized trienzymatic sequence.

Chitosan and polylactide films are good host matrices for bioactive containers because of their biocompatibility and abundance. Ethyl cellulose microspheres loaded with ciprofloxacin were dispersed uniformly in a chitosan film having

round shape and diameter between 0.5 and 3 µm (Fig. 9).^{53,54}

Two steps were adopted in the film-forming process. The first was formation of the drug-loaded ethyl cellulose microspheres in chitosan solution by solvent removal/solvent evaporation methods. Then, the composite films were made by casting and solvent evaporation. As a result, these drug-loaded round ethyl cellulose microspheres dispersed asymmetrically in the chitosan film and improved the release time. The drug was stable in the blending films, which expressed good cytocompatibility.

The release of bupivacaine and cytarabine was demonstrated for albumin containers in a poly(lactide-co-glycolide) film.^{55,56} A matrix formed by bupivacaine-loaded microspheres in a poly(lactide-co-glycolide) film was prepared in order to improve the controlled release of the drug *in vitro* in phosphate buffer at 37 °C in the absence and in the presence of protease. The maximum release of bupivacaine from free microspheres was found after 28 ± 2 h; the microspheres disappear after 8 days. Inclusion of bupivacaine-loaded microspheres in a poly(lactide-co-glycolide) film caused a slower release of the drug, up to 18 days. The film matrix protected bupivacaine-loaded microspheres from degradation, which took place at 20 days. A slower kinetic release of the drug was obtained from composite films, although only 80% of the included cytarabine was released up to day 7.

A new one-batch approach to fabrication of a biodegradable Ca-alginate film with embedded vitamin E loaded microspheres, that could be used for planar dermal drug delivery, was demonstrated by Borodina *et al.*⁵⁷ Stable vitamin E microspheres, coated with gum acacia, were produced from a two-phase liquid system. Gum acacia (GA), as a shell material, fulfils the following essential conditions: (1) It is a natural, harmless and environmentally-friendly polymer; (2) it is widely used internally to treat inflammation of the intestinal mucosa, and externally to cover inflamed surfaces.⁵⁸ FTIR spectroscopy indicates an interaction between biopolymer functional groups induced by ultrasonication. Confocal laser fluorescence scanning microscopy, scanning electron microscopy and atomic force microscopy

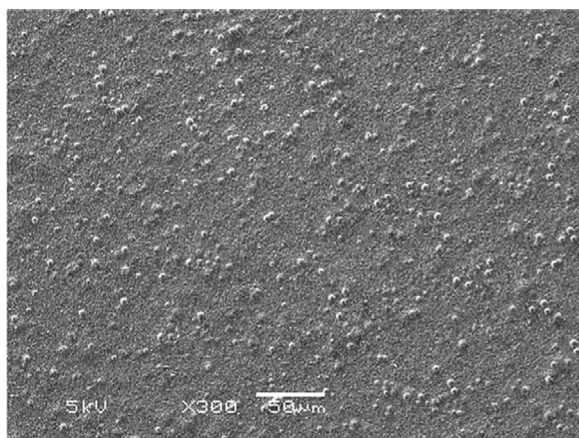


Fig. 9 SEM images of ethyl cellulose microspheres incorporated into a chitosan film at 40 °C.⁵³

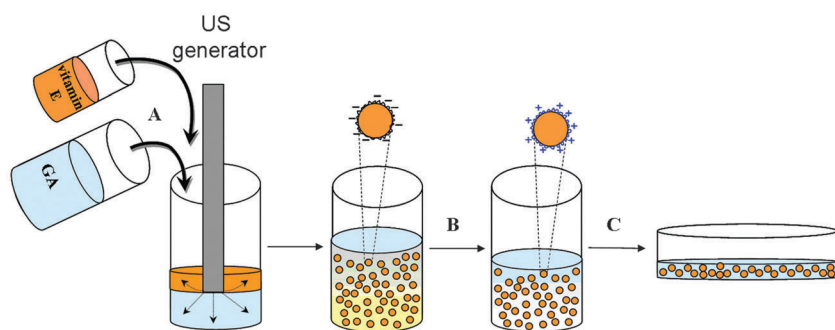


Fig. 10 Schematic demonstration of vitamin E microsphere preparation: (a) emulsification of vitamin E in gum acacia solution by ultrasonication; (b) poly-L-lysine adsorption; (c) the microsphere embedding into polymer Ca-alginate film.⁵⁷

proved a homogeneous microsphere distribution within the Ca-alginate polymer film. The kinetics of *in vitro* vitamin E release found for the polymer film with entrapped microspheres was much more sustained (100% in 96 h) compared to the polymer film with vitamin E embedded in the free state (100% in 5 h).

GA capsules with entrapped vitamin E were synthesized by ultrasound treatment as shown in Fig. 10. The O/W emulsion was formed by mixing 20 ml of 1 wt% aqueous GA solution and 2 ml of vitamin E. The fine emulsion was fabricated by high-intensity ultrasound. The bottom of the ultrasonic horn was immersed in the preformed coarse emulsion, and the systems were sonicated at 23 W cm^{-2} and 20 kHz frequency for 2 min. The microcontainers loaded with oils (soybean oil, hexane or cyclohexane) were prepared following the same procedure, but soybean oil, hexane or cyclohexane were added instead of vitamin E. This intensity of ultrasound did not significantly influence the vitamin E chemical structure; the IR spectrum of vitamin E after encapsulation did not undergo remarkable change and had the same peaks as the spectrum of untreated vitamin E. Vitamin E filled microcapsules were embedded into the Ca-alginate film. Alginate was selected here as a natural biodegradable polysaccharide widely used to prepare various bioactive delivery systems.⁵⁹ The capsules were directly added to sodium alginate solution under stirring, followed by Ca-alginate gel formation (Fig. 10c). This procedure allows the avoidance of hazardous conditions during film preparation (such as high temperature, non-physiological pH, organic solvents, *etc.*),

which is of great importance to retain maximum activity of the bioactive substances.

A homogeneous distribution of the non-aggregated capsules was observed in the Ca-alginate film. The average number density of the spheres calculated from analysis of the confocal microscopy images is $1.31 \times 10^5 \text{ mm}^{-2}$. This simple and versatile procedure requires no use of high temperature, toxic organic solvents or non-physiological pH. The system is attractive due to its ability to encapsulate various unstable bioactive substances by a simple and reproducible procedure. By using different polymers for the microcontainer and film formation, these bioactive coatings could open new applications in many fields, particularly these concerning medicine, pharmacy and cosmetics.

The surface-mediated layer-by-layer self-assembly of hydrogen-bonding water-soluble polymer capsules and hydrogels was demonstrated by Sukhishvili *et al.*^{60,61} The capsules are responsive to environmental stimuli, such as pH, temperature or ionic strength. Through manipulating properties of multilayers at the nanoscale level during self-assembly, a whole range of new feedback active materials can be produced. The promising example of these materials is as polymeric hollow particles and layers which may be used for controlled delivery of drugs or other functional molecules (pesticides, fertilizers or fragrances).

Summary & outlook

The concept of novel active coatings based on the implementation of micro- or nanocontainers filled with active agent into the coating matrix is successfully

proven by numerous examples showing good performance of these coatings on the laboratory scale. The most important feature of the new coating generation is their self-response to external stimuli. After the impact is stopped, the triggering effect is usually relinquished and the rate of release of encapsulated material reduces to zero. The contingent reproducibility between active and passive state of the container ensures the low consumption of active agents.

Further transfer of this approach to the technology level is, however, connected with some restrictions dictated by industrial requirements for the coating. High ratio of container size and the coating thickness can result in the loss of physical integrity of the coating matrix and, therefore, in the failure of its passive properties. This limits the maximal container size and their content in the coating formulation. The other essential issue is the very complex chemical interplay between materials of the substrate, containers, coating matrix and active agent chosen for the encapsulation. The compositions of all elements of the feedback active system have to provide good physicochemical compatibility expressed in terms of such properties as dispersibility and colloidal stability of initial fluid coating formulation, adhesion between containers and host matrix, as well as between matrix and substrate in the cured state. Following this line, large micrometric containers with polymeric shells are, for example, suitable for coating formulations on the basis that organic solvents after curing yield relatively thick coatings. By contrast, submicrometer or nanoscale containers with mesoporous ceramic cores (scaffolds) could be pertinent for water-borne coatings with moderate or small thickness.

On the other hand, the demonstrated universal approach for the fabrication of active coatings is also a great challenge to develop multifunctional organic and composite nanocontainers able to encapsulate active material, retain it in the inner volume for a long period, and immediately release it on demand. A lot of research work still remains, especially in better understanding of the detailed mechanism of shell permeation and of the structure of the inner voids. Notwithstanding to the fact that perspectives of nanocontainer applications have already

been demonstrated, the necessary up-scaling technologies for fabrication of micro- and nanocontainers in large quantities are not yet comprehensively developed.

Acknowledgements

The authors thank Dr M. Hollamby, Dr Y.-S. Han, Dr D. Grigoriev, M. Haase, D. Borisova and A. Latnikova from Department of Interfaces, Max-Planck Institute of Colloids and Interfaces, Potsdam, Germany, for their help in conducting experimental work. EU FP7 Program (MUST project) and BMBF ForMaT program (INTENSA Project) are acknowledged for financial support.

Notes and references

- S. R. White, N. R. Sottos, P. H. Geubelle, J. S. Moore, M. R. Kessler, S. R. Sriram, E. N. Brown and S. Viswanathan, *Science*, 2001, **409**, 794.
- C. J. Hansen, W. Wu, K. S. Toohey, N. R. Sottos, S. R. White and J. A. Lewis, *Adv. Mater.*, 2009, **21**, 4143.
- D. G. Shchukin and H. Möhwald, *Small*, 2007, **3**, 926.
- M. L. Zheludkevich, S. K. Poznyak, L. M. Rodrigues, D. Raps, T. Hack, L. F. Dick, T. Nunes and M. G. S. Ferreira, *Corros. Sci.*, 2010, **52**, 602.
- D. V. Andreeva, D. Fix, H. Möhwald and D. G. Shchukin, *Adv. Mater.*, 2008, **20**, 2789.
- G. B. Sukhorukov and H. Möhwald, *Trends Biotechnol.*, 2007, **25**, 93.
- A. D. Price, A. N. Zelikin, Y. J. Wang and F. Caruso, *Angew. Chem., Int. Ed.*, 2009, **48**, 329–332.
- D. G. Shchukin, E. Ustinovich, G. B. Sukhorukov, H. Möhwald and D. V. Sviridov, *Adv. Mater.*, 2005, **17**, 468.
- D. G. Shchukin, G. B. Sukhorukov, R. R. Price and Y. M. Lvov, *Small*, 2005, **1**, 510.
- Y. M. Lvov, D. G. Shchukin, H. Möhwald and R. R. Price, *ACS Nano*, 2008, **2**, 814.
- N. Dong, A. K. Agarwal, D. J. Beebe and H. R. Jiang, *Nature*, 2006, **442**, 551.
- K. Ishihara and T. Konno, *Biomaterials*, 2007, **28**, 1770.
- S. Gupta and S. P. Moulik, *J. Pharm. Sci.*, 2008, **97**, 22.
- A. S. Narang, D. Delmarre and D. Gao, *Int. J. Pharm.*, 2007, **345**, 9.
- G. Schneider and G. Decher, *Nano Lett.*, 2004, **4**, 1833.
- S. S. Shiratori and M. F. Rubner, *Macromolecules*, 2000, **33**, 4213.
- D. G. Shchukin and G. B. Sukhorukov, *Adv. Mater.*, 2004, **16**, 671.
- S. K. Mehta, G. Kaur and K. K. Bhasin, *Pharm. Res.*, 2007, **25**, 227.
- M. Javier, P. de Pino, M. F. Bedard, A. G. Skirtach, G. B. Sukhorukov and W. J. Parak, *Langmuir*, 2008, **24**, 12517.
- X. Tao, J. B. Li and H. Möhwald, *Chem.–Eur. J.*, 2004, **10**, 3397.
- D. G. Shchukin and D. V. Sviridov, *J. Photochem. Photobiol., C*, 2006, **7**, 23.
- A. Fery and R. Weinkamer, *Polymer*, 2007, **48**, 7221.
- K. Köhler, D. G. Shchukin, H. Möhwald and G. B. Sukhorukov, *J. Phys. Chem. B*, 2005, **109**, 18250.
- A. A. Antipov and G. B. Sukhorukov, *Adv. Colloid Interface Sci.*, 2004, **111**, 49.
- D. G. Shchukin, K. Köhler and H. Möhwald, *J. Am. Chem. Soc.*, 2006, **128**, 4560.
- E. N. Brown, S. R. White and N. R. Sottos, *J. Mater. Sci.*, 2004, **39**, 1703.
- X. Liu, J. K. Lee, S. H. Yoon and M. R. Kessler, *J. Appl. Polym. Sci.*, 2006, **101**, 1266.
- C. Suryanarayana, R. K. Chowdoji and D. Kumar, *Prog. Org. Coat.*, 2008, **63**, 72.
- Z. Liqun, Z. Wei, L. Feng and Y. He, *J. Mater. Sci.*, 2004, **39**, 495.
- K. L. Mittal, *Silanes and other Coupling Agents*, VSP, Utrecht, 1992.
- A. Latnikova, D. O. Grigoriev, J. Hartmann, H. Möhwald and D. G. Shchukin, *Soft Matter*, 2011, **7**, 369.
- D. O. Grigoriev, T. Bukreeva, H. Möhwald and D. G. Shchukin, *Langmuir*, 2008, **24**, 999.
- K. Aramaki, *Corros. Sci.*, 2003, **45**, 451.
- J. Li and H. D. H. Stöver, *Langmuir*, 2010, **26**, 15554.
- M. F. Haase, D. Grigoriev, H. Möhwald, B. Tiersch and D. G. Shchukin, *J. Phys. Chem. C*, 2010, **114**, 17304.
- M. F. Haase, D. Grigoriev, H. Möhwald, B. Tiersch and D. G. Shchukin, *Langmuir*, 2011, **27**, 74.
- D. G. Shchukin, M. L. Zheludkevich, K. A. Yasakau, S. V. Lamaka, M. G. S. Ferreira and H. Möhwald, *Adv. Mater.*, 2006, **18**, 1672.
- M. L. Zheludkevich, D. G. Shchukin, K. A. Yasakau, H. Möhwald and M. G. S. Ferreira, *Chem. Mater.*, 2007, **19**, 402.
- Y. Lvov, R. Price, B. Gaber and I. Ichinose, *Colloids Surf., A*, 2002, **198–200**, 375.
- R. Price, B. Gaber and Y. Lvov, *J. Microencapsulation*, 2001, **18**, 713.
- D. Fix, D. Andreeva, D. G. Shchukin, Y. M. Lvov and H. Möhwald, *Adv. Funct. Mater.*, 2009, **19**, 1720.
- E. Abdullayev, R. Price, D. Shchukin and Y. Lvov, *ACS Appl. Mater. Interfaces*, 2009, **1**, 1437.
- E. Abdullayev and Y. Lvov, *J. Mater. Chem.*, 2010, **20**, 6681.
- D. Borisova, H. Möhwald and D. G. Shchukin, *ACS Nano*, 2011, **5**, 1939.
- E. V. Skorb, D. Fix, D. V. Andreeva, H. Möhwald and D. G. Shchukin, *Adv. Funct. Mater.*, 2009, **19**, 2373.
- D. G. Shchukin and H. Möhwald, *Adv. Funct. Mater.*, 2007, **17**, 1451.
- J. Kecht, A. Schlossbauer and T. Bein, *Chem. Mater.*, 2008, **20**, 7207.
- L. Jie, L. Monty, I. Z. Jeffrey and T. Fuyuhiko, *Small*, 2007, **3**, 1341.
- M. J. Hollamby, D. Fix, I. Dönch, D. Borisova, H. Möhwald and D. G. Shchukin, *Adv. Mater.*, 2011, **23**, 1361.
- D. Volodkin, Y. Amtz, P. Schaaf, H. Möhwald, J. C. Voegel and V. Ball, *Soft Matter*, 2008, **4**, 122.
- F. Cavalieri, A. Postma, L. Lee and F. Caruso, *ACS Nano*, 2009, **3**, 234.
- P. E. Michel, S. M. Gautier-Sauvigne and L. J. Blum, *Talanta*, 1998, **47**, 169.
- P. J. Shi, Y. B. Li and L. Zhang, *Carbohydr. Polym.*, 2008, **72**, 490.
- P. J. Shi, Y. Zuo, Q. Zou, J. Shen, L. Zhang, Y. B. Li and Y. S. Morsi, *Int. J. Pharm.*, 2009, **375**, 67.
- M. V. Bernardo, M. D. Blanco, C. Gomez, R. Olmo and J. M. Teijon, *J. Microencapsulation*, 2000, **17**, 721.
- C. Gomez, M. D. Blanco, M. V. Bernardo, R. Olmo, E. Muniz and J. M. Teijon, *Eur. J. Pharm. Biopharm.*, 2004, **57**, 225.
- T. Borodina, D. Grigoriev, E. Markvicheva, H. Möhwald and D. G. Shchukin, *Adv. Eng. Mater.*, 2011, **13**, B123.
- A. M. Gamal el-din, A. M. Mostafa, O. A. Al-Shabanah, A. M. Al-Bekairi and M. N. Nagi, *Pharmacol. Res.*, 2003, **48**, 631.
- M. Rajaonarivony, C. Vauthier, G. Couarraze, F. Puisieux and P. Couvreur, *J. Pharm. Sci.*, 1993, **82**, 912.
- V. Kozlovskaya, A. Shamaev and S. A. Sukhishvili, *Soft Matter*, 2008, **4**, 1499.
- E. Kharlampieva, I. Erel-Unal and S. A. Sukhishvili, *Langmuir*, 2007, **23**, 175.